

Electronic Supplementary Information

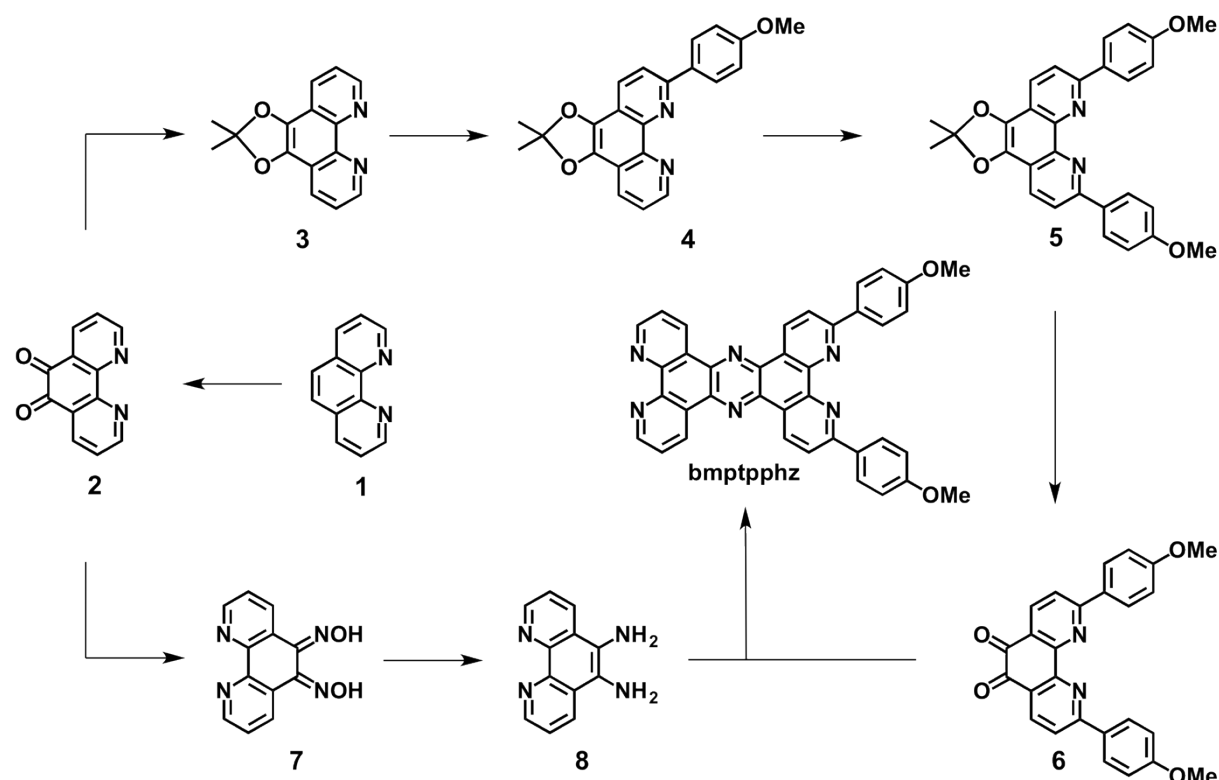
Tuning of photocatalytic activity by creating a tridentate coordination sphere for palladium

M. G. Pfeffer, L. Zedler, S. Kupfer, M. Paul, M. Schwalbe, K. Peuntinger, D. M. Guldi, J. Guthmüller, J. Popp, S. Gräfe, B. Dietzek, S. Rau*

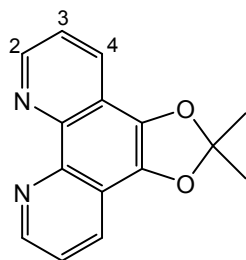
Synthesis and Characterization

1,10-phenanthroline-mono-hydrate (phen), NH_4PF_6 , 2-nitropropane, *n*-butyllithium, MnO_2 , Celite, trifluoroacetic acid and all other materials were of commercial grade and used without further purification. 4,4'-di-*tert*-butyl-2,2'-bipyridine (tbbpy), $[(\text{tbbpy})_2\text{RuCl}_2]$, 1,10-phenanthroline-5,6-dione (phenO₂) and 1,10-phenanthroline-5,6-diamine (phen(NH₂)₂) were prepared according to literature methods.^{1,2,3,4,5,6,7}

¹H-NMR signals were either assigned based on literature^{8,7} or by H,H-COSY experiments.



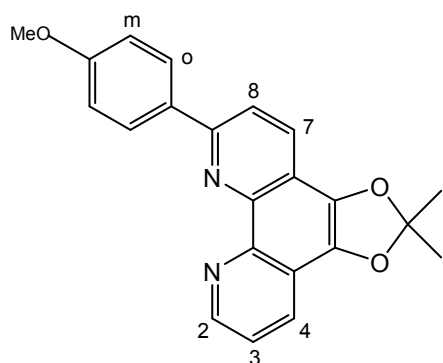
Scheme S1. Synthetic route for the novel **bmptpphz** ligand.



M = 252.3 g/mol

C₁₅H₁₂N₂O₂

Compound 3. 1,10-phenanthroline-5,6-dione (2.5 g, 11.89 mmol) **2** and 2-nitropropane (100 ml, 1.11 mol) were suspended in acetonitrile/water (75 ml/75 ml) and degassed with argon. Afterwards an aqueous degassed solution of Na₂CO₃ (2 M, 6 ml, 1 equiv) was added. The reaction mixture was then heated to reflux for 5 h under argon atmosphere. After cooling to room temperature the product was extracted with dichloromethane. The combined organic extracts were dried over MgSO₄, filtered and dried using the rotary evaporator. The crude product was dissolved in a small amount of toluene, unsolvable residues were filtrated and adding n-hexane precipitated the product. The product was filtered off and the remaining solution was dried once more using the rotary evaporator, dissolved in a small amount of toluene, compounded with n-hexane and filtered. The combined solid fractions were finally dried *in vacuo* yielding the pure product as a yellowish solid. Yield = 58% (1.74 g); M (C₁₅H₁₂N₂O₂) = 252.3 g mol⁻¹; MS (FD in CH₂Cl₂): m/z = 254 [M+H]⁺; ¹H-NMR (270 MHz, CDCl₃, 295 K): δ = 9.07 (dd, 2 H, *J* = 1.76 Hz and 4.31 Hz, 2), 8.24 (dd, 2 H, *J* = 1.74 Hz and *J* = 8.23 Hz, 4), 7.60 (dd, 2 H, *J* = 4.34 Hz and *J* = 8.22 Hz, 3), 1.25 (s, 6 H, *J* = 8.0 Hz, Me) ppm;

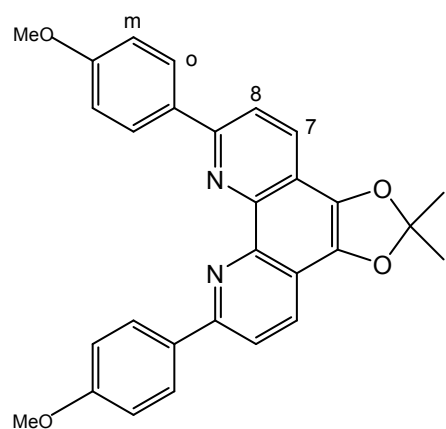


M = 358.39 g/mol

C₂₂H₁₈N₂O₃

Compound 4. Under argon atmosphere, *n*-butyllithium (8.62 ml, 13.8 mmol, 1.6 M in hexane) was added within 10 min dropwise at -78 °C to a degassed solution of *p*-bromoanisole (1.72 ml, 13.8 mmol) in dry tetrahydrofuran (30 ml). The reaction mixture was stirred for 15 min until a solution of **3** (1.74 g, 6.7 mmol) in dry tetrahydrofuran (25 ml) was slowly added. The mixture was stirred for additional 2 h at -78 °C and subsequently MeOH

(9 ml) was added. The solution was allowed to warm to room temperature and the solvent was removed by rotary evaporation. The residue was solved in dichloromethane/toluene (75 ml/75 ml) and mixed with activated MnO₂ (4.37 g) to rearomatize the crude product. After 12 h of stirring, the suspension was filtered through Celite, which was washed with dichloromethane. The combined organic fractions were dried using rotary evaporation and the residue was dissolved in a small amount of acetone, precipitated by adding *n*-heptane and dried *in vacuo*. Yield = 79 % (1.88 g); M (C₂₂H₁₈N₂O₃) = 358.4 g mol⁻¹; Anal. Calcd for C₂₂H₁₈N₂O₃: C = 71.42, H = 4.79, N = 11.10; found: C = 70.30, H = 4.60, N = 10.78; MS (FAB in 3-nitrobenzyl alcohol): *m/z* = 359 [M+H]⁺; ¹H-NMR (270 MHz, CDCl₃, 295 K): δ = 9.13 (dd, 1 H, *J* = 1.78 and *J* = 4.02 Hz, 2), 8.24-8.36 (m, 4 H, 4 + 7 + o), 8.05 (d, 1 H, *J* = 8.60 Hz, 8), 7.61 (dd, 1 H, *J* = 4.43 and *J* = 8.26 Hz, 3), 7.05 (d, 2 H, *J* = 8.90 Hz, m), 3.88 (s, 3 H, OMe), 1.87 (s, 6 H, Me) ppm; ¹³C-NMR (CDCl₃, 100 MHz, 295 K): δ = 160.79, 154.91, 147.85, 142.35, 142.20, 136.77, 136.00, 132.40, 129.17, 128.79, 128.22, 122.58, 120.74, 119.91, 118.71, 116.76, 114.23, 55.48, 26.18 ppm;

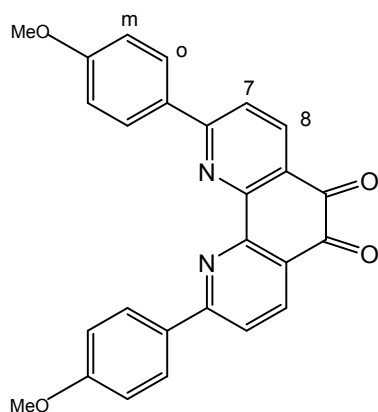


M = 464.51 g/mol

C₂₉H₂₄N₂O₄

Compound 5. To a degassed solution of *p*-bromoanisole (1.3 ml, 10.4 mmol) in dry tetrahydrofuran (40 ml) *n*-butyllithium (6.54 ml, 10.4 mmol, 1.6 M in hexane) was added dropwise over 10 min at -78 °C under argon. The reaction mixture was stirred for 15 min until a solution of **4** (1.88 g, 5.27 mmol) in dry tetrahydrofuran (40 ml) was slowly added. Afterwards the solution was slowly warmed to room temperature and stirred over night. Subsequently water (0.5 ml) was added to the deep-purple mixture. The resulting reddish solution was concentrated to dryness and then solved in dichloromethane (500 ml). After addition of MnO₂ (3.5 g) the suspension was stirred over night and filtered through Celite. The solvent was removed using a rotary evaporator and the residue was suspended in acetone (200 ml) and stirred for 10 min. The insoluble yellow product was filtered off and washed

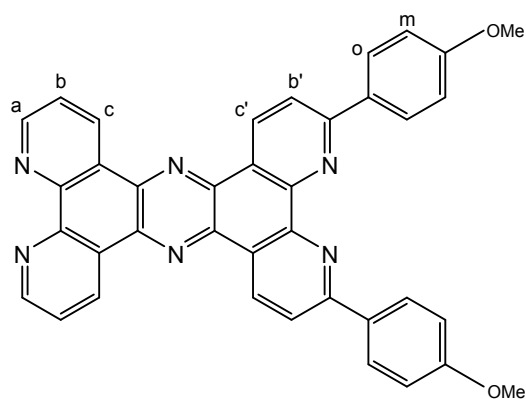
with acetone and diethyl ether. Yield = 48% (1.17 g); M ($C_{29}H_{24}N_2O_4$) = 464.5 g mol⁻¹; Anal. Calcd for $C_{22}H_{18}N_2O_3$: C = 74.98, H = 5.21, N = 6.03; found: C = 73.94, H = 5.06, N = 5.97; MS (FAB in 3-nitrobenzyl alcohol): m/z = 465 [M+H]⁺; ¹H-NMR (CDCl₃, 270 MHz, 275 K): δ = 8.39 (d, 4 H, J = 8.98 Hz, o), 8.25 (d, 2H, J = 8.64 Hz, 7), 8.06 (d, 2 H, J = 8.64 Hz, 8), 7.09 (d, 4 H, J = 8.97 Hz, m), 3.90 (s, 6 H, OMe), 1.87 (s, 6 H, Me) ppm;



M = 422.73 g/mol

$C_{26}H_{18}N_2O_4$

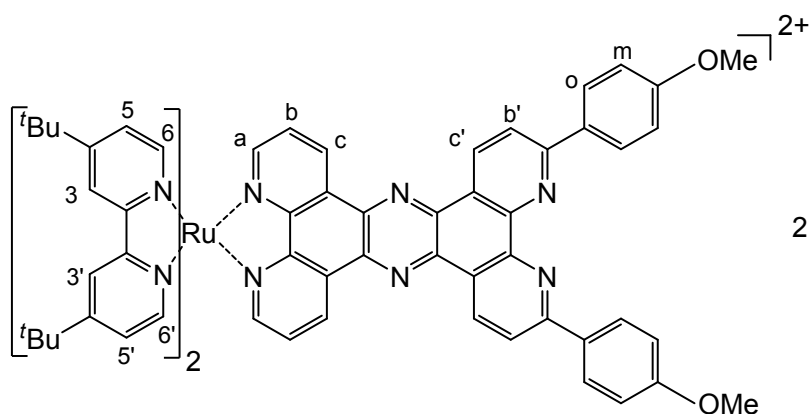
Compound 6. 5 (0.23 g, 0.50 mmol) was solved in water/trifluoroacetic acid (33 ml/66 ml). After 5 h of stirring at 50 °C the initially reddish solution turned to orange. The solvent was removed and the residue solved in dichloromethane and extracted with an aqueous solution of NaHCO₃ (1 M). The organic fraction was separated washed with water, dried over MgSO₄ and filtered. The solvent was removed, the residue suspended in toluene and stirred for 10 min. The solid was filtered off, washed with diethyl ether and dried *in vacuo*, yielding the pure bright orange product. Yield = 86% (0.18 g); M ($C_{26}H_{18}N_2O_4$) = 422.7 g mol⁻¹; ¹H-NMR (270 MHz, CDCl₃, 295 K): δ = 8.48 (d, 2 H, J = 8.34 Hz, 7), 8.34 (d, 4 H, J = 8.85 Hz, o), 7.93 (d, 2 H, J = 8.34 Hz, 8), 7.09 (d, 4 H, J = 8.92 Hz, m), 3.92 (s, 6 H, OMe) ppm;



M = 596.64 g/mol

C₃₈H₂₄N₆O₂

bmptpphz. To a boiling solution of **6** (0.46 g, 1.08 mmol) in methanol (250 ml) phen(NH₂)₂ **8** (0.31 g, 1.49 mmol) was added portionwise over 2 h. The mixture was refluxed for 8 h, whereby the bright yellow product precipitated. The product was filtered off and washed with water, methanol and acetone and dried *in vacuo*. Yield = 76% (0.49 g); M (C₃₈H₂₄N₆O₂) = 596.6 g mol⁻¹; MS (DEI in acetonitrile + trifluoroacetic acid): m/z = 596 [M-H]⁻; ¹H-NMR (270 MHz, CDCl₃ + trifluoroacetic acid, 295 K): δ = 10.21 (d, 2 H, J = 7.96 Hz, c), 10.10 (d, 2 H, J = 8.87 Hz, c'), 9.36 (d, 2 H, J = 4.87 Hz, a), 8.64 (d, 2 H, J = 8.86 Hz, b'), 8.36 (dd, 2 H, J = 5.20 and J = 8.33 Hz, b), 8.25 (d, 4 H, J = 8.69 Hz, o), 7.27 (d, 4 H, J = 8.71 Hz, m), 4.01 (s, 6 H, OMe) ppm;



2 PF₆⁻

M = 1526.7 g/mol

C₇₄H₇₄N₁₀O₂RuP₂F₁₂

Ru(bmptpphz). The ligand **bmptpphz** (0.49 g, 0.82 mmol) was suspended in ethanol/water (100 ml/100 ml) and heated to reflux. Afterwards [(tbbpy)₂RuCl₂] (0.60 g, 0.85 mmol) in ethanol/water (50 ml/50 ml) was added during 1 h. The orange-brown suspension was refluxed for 18 h more and subsequently filtered while hot to remove unreacted ligand. Afterwards the solution was concentrated under reduced pressure using a rotary evaporator and the crude product was precipitated by adding 100 ml of an aqueous solution of NH₄PF₆ (0.80 g, 5.0 mmol). The precipitated brown-reddish solid was filtered off and washed with water, diethyl ether and dried *in vacuo*.

Finally, the ruthenium complex was purified by column chromatography on silica (dichloromethane/methanol 1:1 v/v). The product elutes as first band.

Yield = 78% (1.0 g); $M(C_{74}H_{72}F_{12}N_{10}O_2P_2Ru) = 1524.4 \text{ g mol}^{-1}$; MS (FD in acetonitrile): $m/z = 1380 [M-PF_6]^+$; 1H -NMR (400 MHz, CD_3CN , 295 K, $c = 0.01 \text{ M}$): $\delta = 9.42$ (d, 2 H, $J = 8.18 \text{ Hz}$, c), 9.19 (d, 2 H, $J = 8.82 \text{ Hz}$, c'), 8.63 (d, 2 H, $J = 1.86 \text{ Hz}$, 3'), 8.60 (d, 2 H, $J = 1.81 \text{ Hz}$, 3), 8.13 (dd, 2 H, $J = 4.96, 1.25 \text{ Hz}$, a), 8.07 (d, 4 H, $J = 8.57 \text{ Hz}$, o), 8.01 (d, 2 H, $J = 8.54 \text{ Hz}$, b'), 7.92 - 7.64 (m, 6H, 6', b, 6), 7.55 (dd, 2 H, $J = 5.90, 2.14 \text{ Hz}$, 5'), 7.41 (d, 2 H, $J = 6.14 \text{ Hz}$, 5), 6.68 (d, 4 H, $J = 8.43 \text{ Hz}$, m), 3.73 (s, 6 H, MeO), 1.51 (s, 18 H, *tert.* Butyl), 1.37 (s, 18 H, *tert.* Butyl) ppm; ^{13}C -NMR (100 MHz, CD_3CN , 295 K): $\delta = 29.58, 29.68, 35.53, 35.58, 55.08, 118.84, 118.87, 121.76, 121.82, 123.93, 124.9, 126.45, 128.27, 129.67, 130.37, 133.03, 133.44, 146.73, 149.25, 151.20, 151.29, 152.75, 156.98, 157.12, 157.26, 161.13, 163.09$ ppm;

Thin Layer Chromatography (TLC)

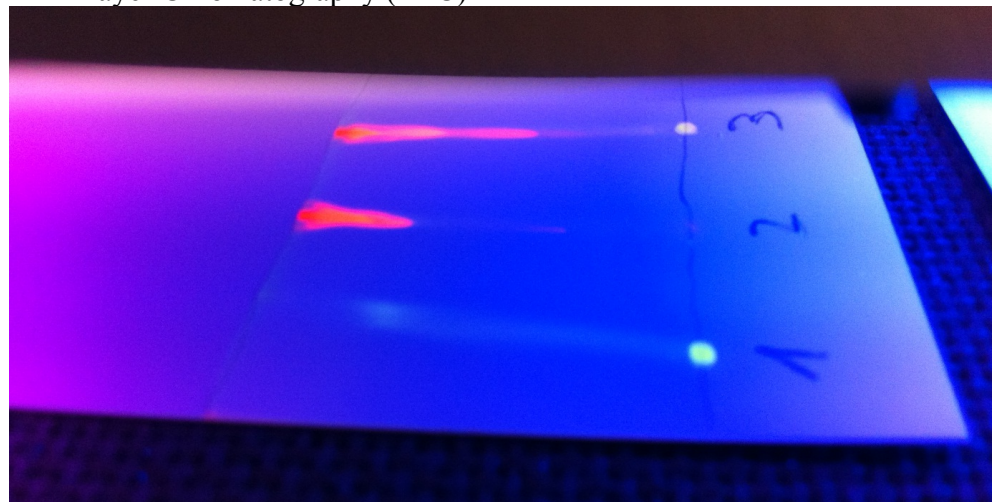
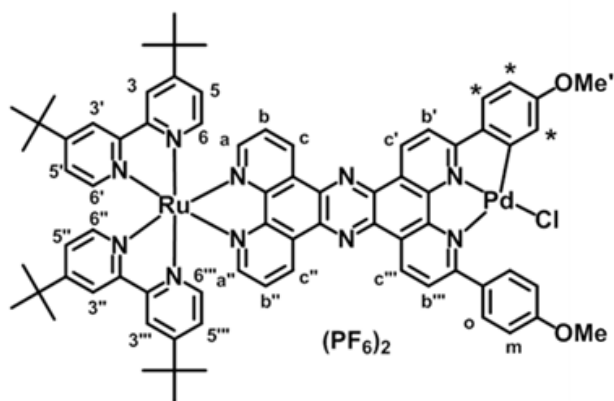
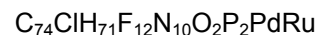


Figure S1. TLC in dichloromethane/methanol (1:1); irradiation with 365 nm UV-Lamp; 1 = pure **bmptpphz**, 2 = **Ru(bmptpphz)**, 3 = mixture of **bmptpphz** and **Ru(bmptpphz)**



$$M = 1665.3 \text{ g mol}^{-1}$$



Ru(bmptpphz)PdCl. 20 mg (0.013 mmol) **Ru(bmptpphz)** were dissolved in 15 ml dichloromethane and 3.9 mg (0.015 mmol) Pd(acn)₂Cl₂ were added. The reaction mixture was stirred for 4 days at room temperature. After 1 day another 1.95 mg (0.0075 mmol) Pd(acn)₂Cl₂ were added. Subsequently, the solvent was evaporated at room temperature and the residue was dissolved acetonitrile and applied to a column with silica as solid phase and washed with water. Afterwards the dinuclear complex was eluted with acetonitrile/water+KNO₃ (saturated) 15:1 v/v. The fractions were combined and the solution was concentrated under reduced pressure at room temperature. Following this, an aqueous solution of NH₄PF₆ (0.08 mmol) was added to precipitate the product, which was finally separated by filtration and washed with water, diethyl ether and dried *in vacuo*.

Yield = 61% (0.013 g); M(C₇₄ClH₇₁F₁₂N₁₀O₂P₂PdRu) = 1665.3 g mol⁻¹; MS (ESI in acetonitrile): m/z = 965.9 [2M-3PF₆]³⁺, 687.4 [M-2PF₆]²⁺, 617.4 [M-2PF₆-PdCl]²⁺; ¹H-NMR (400 MHz, CD₃CN, 295 K, c = 8.5 mM): δ = 9.91 (d, 1H, J = 8.2 Hz, c''), 9.85 (d, 1H, J = 8.4 Hz, c'''), 9.79 (d, J = 8.3 Hz, c), 9.65 (d, 1H, J = 8.7 Hz, c'), 8.60 (s, 2H, 3/3'''), 8.55 (s, 2H, 3'/3''), 8.32 (dd, 1H, J = 5.3, 1.2 Hz, a'), 8.27 (dd, 1H, J = 5.3, 1.2 Hz, a), 8.24 (d, 1H, J = 8.4 Hz, b'''), 8.08 (dd, 1H J = 8.2, 5.4 Hz, b''), 8.02 (dd, 1H, J = 8.2, 5.3 Hz, b), 7.88 (d, 1H, J = 8.9 Hz, b'), 7.85 – 7.73 (m, 4H, 6/6'''/o), 7.70 (d, 1H, J = 6.2 Hz, 6''), 7.66 (d, 1H, J = 6.1 Hz, 6'), 7.58–7.50 (m, 2H, 5/5'''), 7.48 – 7.27 (m, 3H, 5'/5''/*), 7.24 (d, 2H, J = 8.6 Hz, m), 6.19 (s, 1H, *), 5.99 (s, 1H, *), 3.96 (s, 3H, OMe), 3.44 (s, 3H, OMe'), 1.47 (d, 18H, J = 1.9 Hz, *tert.* Butyl), 1.35 (s, 18H, *tert.* Butyl).

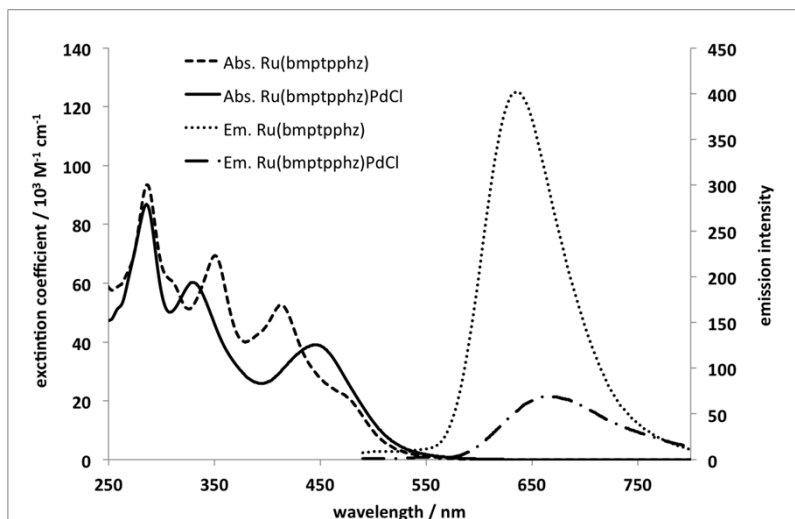


Figure S2. Absorption and emission spectra of **Ru(bmptpphz)** and **Ru(bmptpphz)PdCl** in acetonitrile

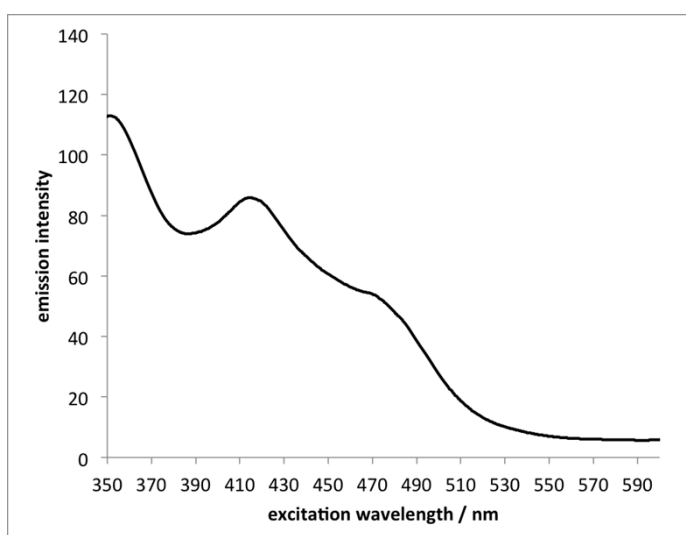


Figure S3. Excitation spectrum of **Ru(bmptpphz)** in acetonitrile, $\lambda_{em} = 632$ nm

	τ_1 [ns]	Ampl. [%]	τ_2 [ns]	Ampl. [%]	τ_3 [ns]	Ampl. [%]	CHISQ
Ru(bmptpphz) 2us 5000counts 1exp	152	100					1.18
Ru(bmptpphz) 2us 5000counts verd 2exp	157	99	5.4	1			1.20
Ru(bmptpphz) 2us 5000counts verd 1exp	156	100					1.59
Ru(bmptpphz) 10us 2500counts inert	930	100					1.07
Ru(bmptpphz) 10us 2500counts inert verd 1exp	934	100					1.15
Ru(bmptpphz) 10us 2500counts inert verd 3exp	939	99	470	0.45	5.2	0.31	1.05

Table S1. Emission lifetimes of **Ru(bmptpphz)** in acetonitrile.

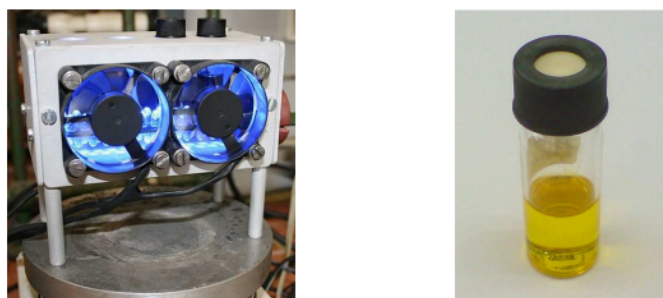


Figure S4. Photomicroreactor with air ventilation and LED irradiation (left) and a commercial available GC vial with septum containing the catalytic mixture (right)

Irradiation time [h]	0	1	2	4	6	8	10	24	39	64	134
Ru(bmptpphz)PdCl	0	0.1±0	0.2±0	0.8±0	1.4±0.2	2.3±0.1	3.3±0.8	11.7±0.4	27.1±4.0	50.3±5.1	32.1±3.0

Table S2. Turnover numbers (TON ± standard error) of **Ru(bmptpphz)PdCl** versus irradiation time

Irradiation time [h]	0	1	2	4	6	18	24	30
Ru(tpphz)PdCl₂	0	0.3±0.2	1.2±0	11.7±0.6	33.4±3.2	143.7±8.6	187.0±7.0	177.6±2.3

Table S3. Turnover numbers (TON ± standard error) of **Ru(tpphz)PdCl₂** versus irradiation time

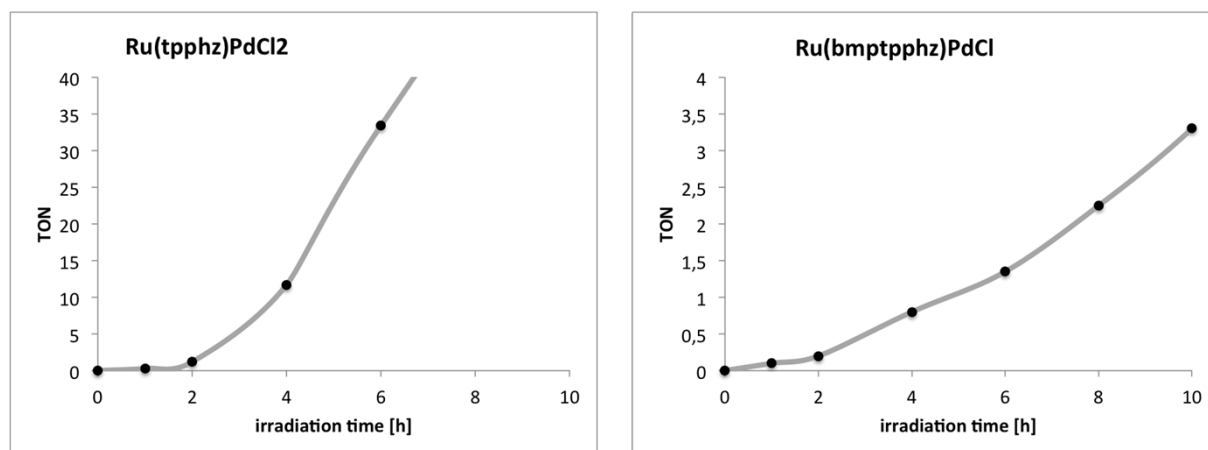


Figure S5. Starting period of photocatalytic hydrogen evolution of **Ru(tpphz)PdCl₂** (left) and **Ru(bmptpphz)PdCl** (right)



Figure S6. Catalytic mixture containing 100 μL of liquid mercury

irradiation time [h]	24	99
TON with addition of Hg	0	0
TON without Hg	12 ± 0.4	33 ± 1.7

Table S4. Summary of the turnover number (TON \pm standard error) after 24 h and 99 h of irradiation with blue LED light (470 nm) for **Ru(bmptpphz)PdCl** with and without addition of 100 μL elemental mercury.

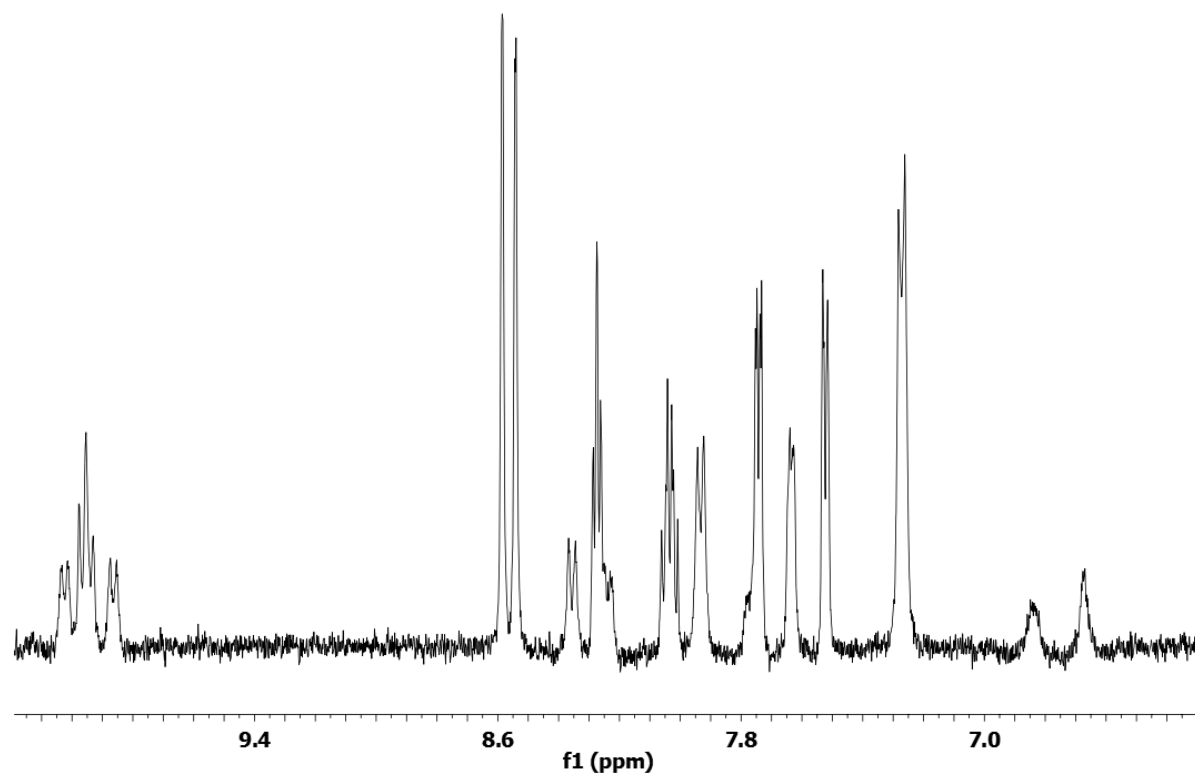


Figure S7. ^1H -NMR spectrum of **Ru(bmptpphz)PdCl** in acetonitrile- d_3 after 7 hours of stirring with liquid Hg. The spectrum shows the set of signals according to the dinuclear complex **Ru(bmptpphz)PdCl**, thus no reaction occurred with liquid Hg.

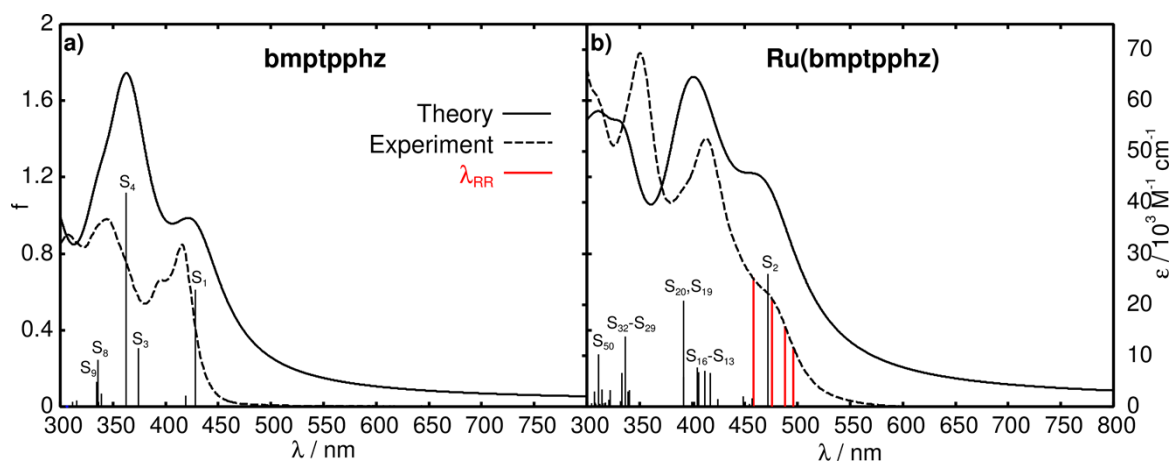


Figure S8. Experimental (dashed line) and theoretical (black line) absorption spectra of **bmptpphz** (a) and **Ru(bmptpphz)** (b) in acetonitrile. The calculated oscillator strengths are represented by black sticks. A Lorentzian function with a full-width at half maximum (FWHM) of 3500 cm^{-1} is employed to broaden the transitions in the simulated spectrum. The four vertical lines in (b) indicate the wavelengths at which the RR measurements are performed (496, 488, 476 and 458 nm).

state	transition	weight / %	E^e / eV	λ / nm	f	λ_{exp} / nm
S ₁	$\pi_{\text{tpphz}}(155) \rightarrow \pi^*_{\text{tpphz}}(156)$	96	2.89	428	0.6119	413
	ILCT					
S ₃	$\pi_{\text{tpphz}}(155) \rightarrow \pi^*_{\text{tpphz}}(157)$	96	3.31	374	0.3066	341
	ILCT					
S ₄	$\pi_{\text{tpphz}}(154) \rightarrow \pi^*_{\text{tpphz}}(157)$	91	3.42	362	1.1184	341
	ILCT					
S ₈	$\pi_{\text{tpphz}}(153) \rightarrow \pi^*_{\text{tpphz}}(156)$	55	3.70	336	0.2450	305
	ILCT	21				
	$\pi_{\text{tpphz}}(155) \rightarrow \pi^*_{\text{tpphz}}(159)$	10				
	ILCT					
S ₉	$\pi_{\text{tpphz}}(155) \rightarrow \pi^*_{\text{tpphz}}(158)$					
	ILCT					
	$\pi_{\text{tpphz}}(154) \rightarrow \pi^*_{\text{tpphz}}(159)$	68	3.71	335	0.1281	305
S ₉	ILCT	19				
	$\pi_{\text{tpphz}}(154) \rightarrow \pi^*_{\text{tpphz}}(158)$					
S ₂₂	ILCT					
	$\pi_{\text{tpphz}}(152) \rightarrow \pi^*_{\text{tpphz}}(157)$	60	4.21	294	0.3610	-
S ₃₀	ILCT					
	$\pi_{\text{tpphz}}(153) \rightarrow \pi^*_{\text{tpphz}}(158)$	53	4.53	274	0.2325	-
	ILCT	10				
	$\pi_{\text{tpphz}}(155) \rightarrow \pi^*_{\text{tpphz}}(161)$	10				
	ILCT	10				
	$\pi_{\text{tpphz}}(153) \rightarrow \pi^*_{\text{tpphz}}(159)$					
S ₃₀	ILCT					
	$\pi_{\text{tpphz}}(148) \rightarrow \pi^*_{\text{tpphz}}(157)$					
S ₃₀	ILCT					

Table S5. Calculated vertical excitation energies (E^e), oscillator strengths (f) and singly-excited configurations of the main excited singlet states and experimental absorption spectrum of **bmptpphz** in acetonitrile. The principal orbitals are depicted on Figure S9.

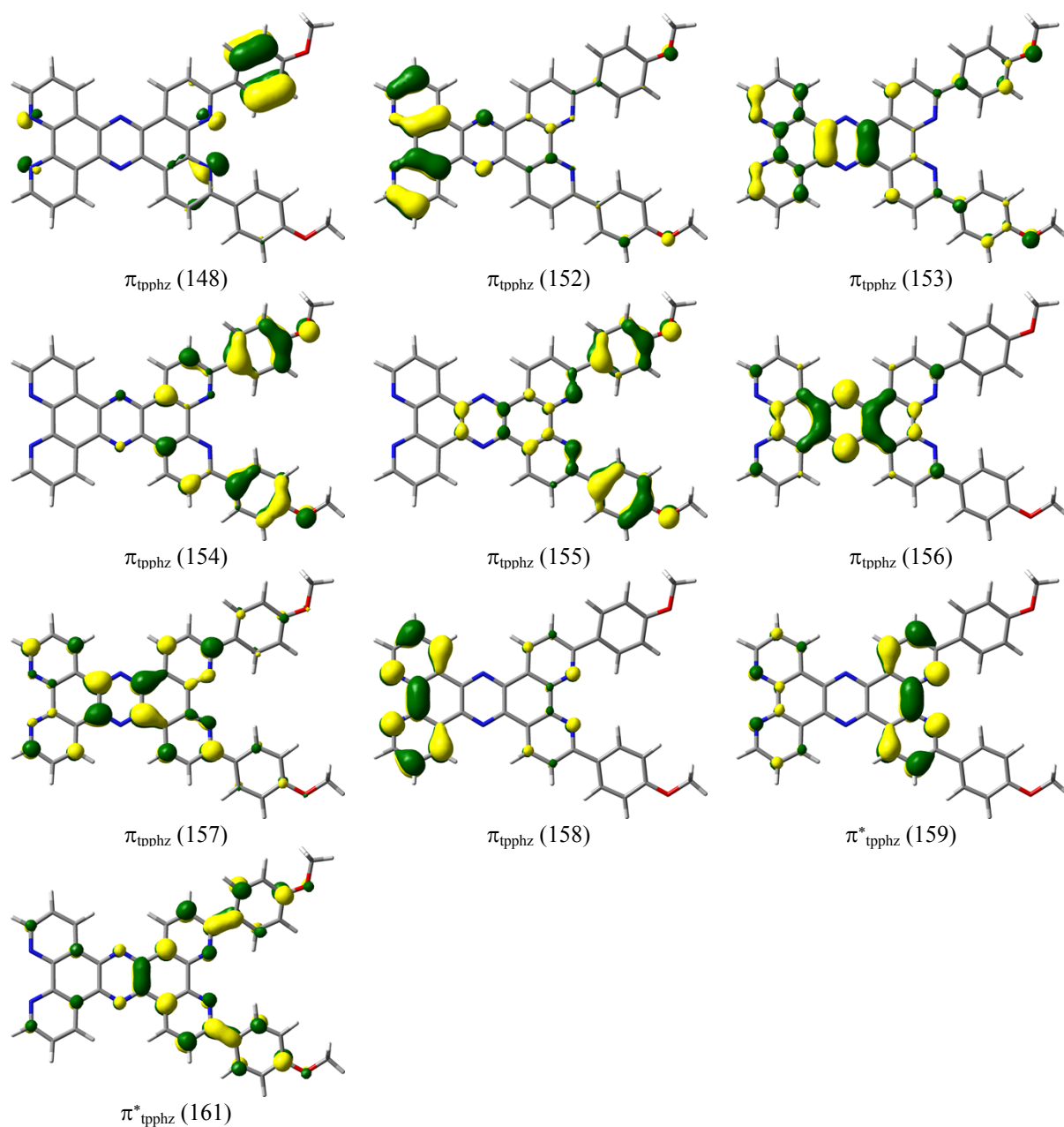


Figure S9. Molecular orbitals involved in the main configurations of the electronic states responsible for the absorption properties of the **bmptpphz** ligand.

state	transition	weight / %	E^e / eV	λ / nm	f	λ_{exp} / nm
S ₂	$\pi_{\text{tpphz}}(308) \rightarrow \pi_{\text{tpphz}}^*(309)$	70	2.63	472	0.6927	416
	ILCT	20				
	$d_{\text{xz}}(304) \rightarrow \pi_{\text{tpphz}}^*(309)$ MLCT					
S ₁₃	$d_{\text{xy}}(305) \rightarrow \pi_{\text{bpy}}^*(313)$ MLCT	28	3.17	417	0.1747	470
	$d_{\text{xz}}(304) \rightarrow \pi_{\text{tpphz}}^*(310)$ MLCT	18				
	$d_{\text{xy}}(305) \rightarrow \pi_{\text{tpphz}}^*(311)$ MLCT	15				
	$d_{\text{xz}}(304) \rightarrow \pi_{\text{bpy}}^*(312)$ MLCT	11				
S ₁₄	$d_{\text{xy}}(305) \rightarrow \pi_{\text{bpy}}^*(312)$ MLCT	51	3.01	412	0.1855	470
	$d_{\text{xz}}(304) \rightarrow \pi_{\text{bpy}}^*(313)$ MLCT	39				
S ₁₅	$\pi_{\text{tpphz}}(308) \rightarrow \pi_{\text{tpphz}}^*(311)$	85	3.05	406	0.1809	470
	ILCT					
S ₁₆	$d_{\text{xy}}(305) \rightarrow \pi_{\text{tpphz}}^*(311)$ MLCT	73	3.07	405	0.2046	470
	$d_{\text{xy}}(305) \rightarrow \pi_{\text{bpy}}^*(313)$ MLCT	13				
S ₁₉	$\pi_{\text{tpphz}}(307) \rightarrow \pi_{\text{tpphz}}^*(310)$	71	3.16	392	0.1539	351
	ILCT	17				
	$\pi_{\text{tpphz}}(307) \rightarrow \pi_{\text{tpphz}}^*(311)$					
	ILCT					
S ₂₀	$\pi_{\text{tpphz}}(307) \rightarrow \pi_{\text{tpphz}}^*(311)$	67	3.16	392	0.5557	351
	ILCT	19				
	$\pi_{\text{tpphz}}(307) \rightarrow \pi_{\text{tpphz}}^*(310)$					
	ILCT					
S ₂₉	$\pi_{\text{tpphz}}(308) \rightarrow \pi_{\text{tpphz}}^*(314)$	34	3.65	340	0.0851	312
	ILCT	23				
	$\pi_{\text{tpphz}}(307) \rightarrow \pi_{\text{tpphz}}^*(314)$	20				
	ILCT					
	$\pi_{\text{tpphz}}(303) \rightarrow \pi_{\text{tpphz}}^*(309)$					
	ILCT					
S ₃₀	$\pi_{\text{tpphz}}(308) \rightarrow \pi_{\text{tpphz}}^*(314)$	46	3.66	339	0.0789	312
	ILCT	18				
	$\pi_{\text{tpphz}}(307) \rightarrow \pi_{\text{tpphz}}^*(314)$	15				
	ILCT					
	$\pi_{\text{tpphz}}(302) \rightarrow \pi_{\text{tpphz}}^*(309)$					
	ILCT					
S ₃₁	$\pi_{\text{tpphz}}(303) \rightarrow \pi_{\text{tpphz}}^*(309)$	56	3.69	336	0.3687	312
	ILCT	14				
	$\pi_{\text{tpphz}}(301) \rightarrow \pi_{\text{tpphz}}^*(309)$					
	ILCT					
S ₃₂	$\pi_{\text{tpphz}}(307) \rightarrow \pi_{\text{tpphz}}^*(314)$	46	3.72	333	0.1760	312

ILCT							
S ₅₀	$\pi_{\text{tpphz}}(307) \rightarrow \pi_{\text{tpphz}}^*(316)$	84	3.98	311	0.2723	312	
ILCT							

Table S6. Calculated vertical excitation energies (E^e), oscillator strengths (f) and singly-excited configurations of the main excited singlet states and experimental absorption spectrum of **Ru(bmptpphz)** in acetonitrile. The principal orbitals are depicted on Figure S10.

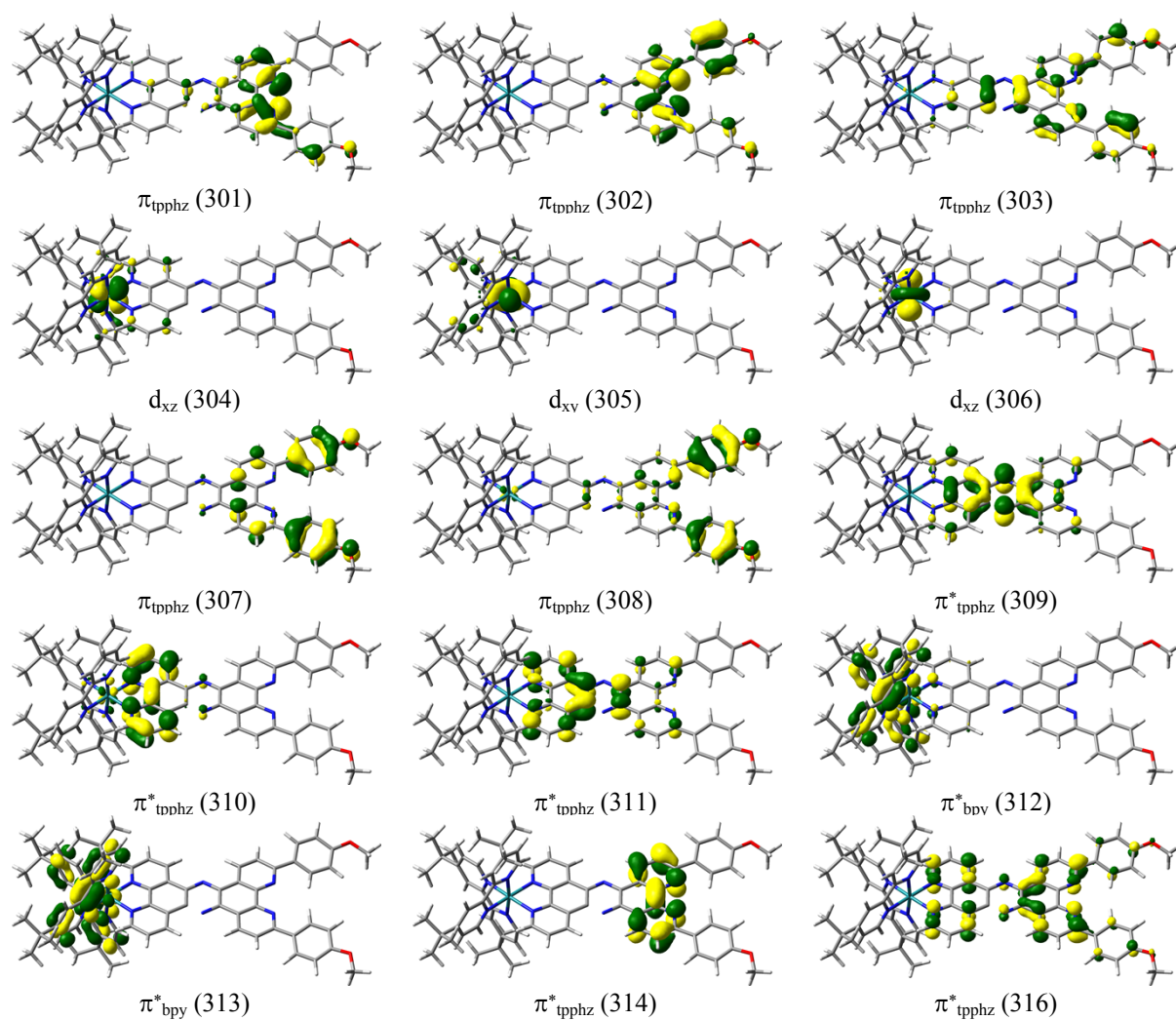


Figure S10. Molecular orbitals involved in the main configurations of the electronic states responsible for the absorption and RR properties of the **Ru(bmptpphz)** complex.

Mode	Character	$\tilde{\nu}_{\text{calc.}} / \text{eV}$	$\tilde{\nu}_{\text{exp.}} / \text{eV}$	$I_{\text{rel.}}(458 \text{ nm})$
268	tpphz	1169	1173	0.15
272	tpphz	1182	1183	0.07
273	tpphz	1197	1200	0.13
284	bpy	1243	1265	0.06
288	tpphz	1258	1265	0.19
289	tpphz	1261	1265	0.05
290	tpphz	1263	1265	0.13
294	bpy	1274	1265	0.05
295	tpphz	1277	1265	0.21
300	tpphz	1293	1282	0.24
302	tpphz	1301	1282	0.19
307	tpphz	1310	1282	0.12
308	bpy	1311	1282	0.06
310	tpphz	1315	1282	0.08
311	tpphz	1317	1282	0.52
313	tpphz	1351	1357	0.99
314	tpphz	1353	1357	0.17
325	tpphz	1402	1409	0.19
327	bpy	1410	1428	0.21
336	tpphz	1432	1470	0.73
337	tpphz	1439	1470	0.26
360	bpy	1479	1483	0.16
367	bpy	1485	1483	0.09
376	tpphz	1499	1503	0.28
380	bpy	1542	1538	0.19
381	bpy	1542	1538	0.17
385	tpphz	1553	-	0.08
386	tpphz	1569	1565	0.05
387	tpphz	1574	1565	0.06
388	tpphz	1575	1565	0.23
389	tpphz	1581	1579	0.23
391	tpphz	1589	1579	1.00
396	tpphz	1615	1602	0.34

Table S7. Assignment of the vibrational frequencies (cm^{-1}) and calculated relative RR intensities ($I_{\text{rel.}}$) at an excitation wavelength of 458 nm and using shifted singlet excitation energies of **Ru(bmptpphz)**. The theoretical frequencies were scaled by a factor of 0.97.

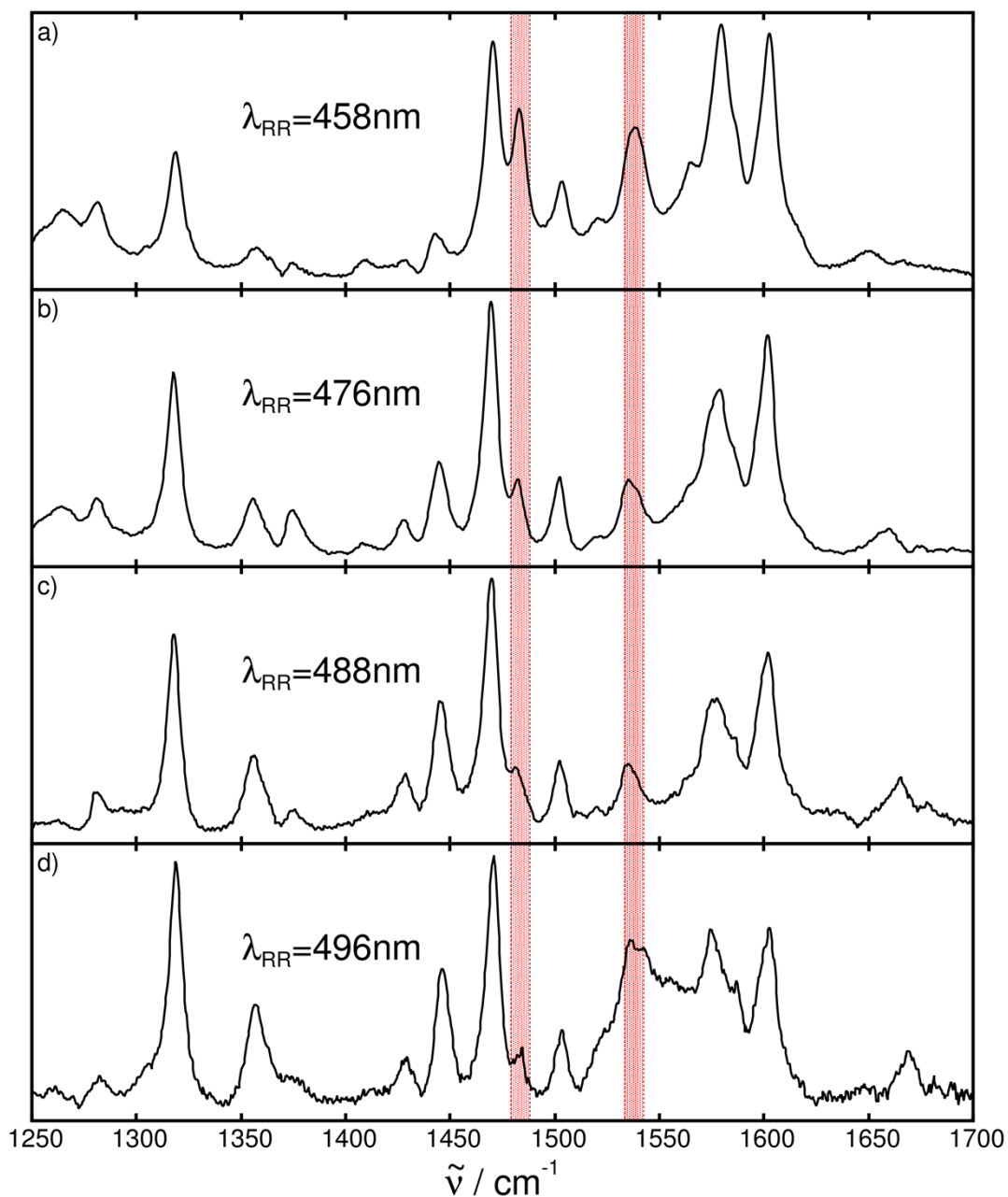


Figure S11. Resonance Raman spectra of **Ru(bmptpphz)** ($c = 1 \times 10^{-4}$ M) in acetonitrile/water (5 v%) at different excitation wavelengths. The red bars indicate to Raman features associated to the bipyridine ligands.

¹ S. Rau, B. Schäfer, D. Gleich, E. Anders, M. Rudolph, M. Friedrich, H. Görls, W. Henry and J. G. Vos, *Angew. Chem., Int. Ed.*, 2006, 45, 6215

² (a) J. Bolger, A. Gourdon, E. Ishow and J.-P. Launay, *J. Chem. Soc., Chem. Commun.*, 1995, 1799–1800; (b) J. Bolger, A. Gourdon, E. Ishow and J.-P. Launay, *Inorg. Chem.*, 1996, 35, 2937–2944

-
- ³ M. Yamada, Y. Tanaka, Y. Yoshimoto, S. Kuroda and I. Shima, Bull. Chem. Soc. Jpn., 1992, 65, 1006–1011
- ⁴ G. Conte, A. J. Bortoluzzi and H. Gallardo, Synthesis, 2006, 23, 3945–3947
- ⁵ P. Comba, R. Krämer, A. Mokhir, K. Naing, E. Schatz, Eur. J. Inorg. Chem. 2006, 4442–4448
- ⁶ M. Karnahl, S. Kriek, H. Görls, S. Tschierlei, M. Schmitt, J. Popp, D. Chartrand, G. S. Hanan, R. Groarke, J. G. Vos and S. Rau, Eur. J. Inorg. Chem., 2009, 4962–4971
- ⁷ S. Rau, B. Schäfer, D. Gleich, E. Anders, M. Rudolph, M. Friedrich, H. Görls, W. Henry and J. G. Vos, Angew. Chem., Int. Ed., 2006, 45, 6215–6218
- ⁸ J. Frey, T. Kraus, V. Heitz and J.-P. Sauvage, Chem. Eur. J. 2007, 13, 7584 – 7594